10
MODERN DIFFRACTION TECHNIQUES FOR TEXTURE ANALYSIS

R.A. Schwarzer

Physikalisches Institut der TU, AG Textur,
D-38678 Clausthal-Z., Germany
e-mail: schwarzer@tu-clausthal.de [*)]

ABSTRACT

Automated Crystal Orientation Measurement (ACOM) enables individual grain orientations to be determined with high speed and accuracy by interpreting backscatter or transmission Kikuchi patterns (SEM or TEM, respectively). The measurement of pole figures in the TEM is an alternative technique with deformed or extremely fine grained materials. In addition, deformation systems can be determined conveniently in the TEM with the assistance of an on-line computer program.

Crystal orientation maps are obtained from ACOM data by assigning colours to the image points, which are specific, e.g., for the grain orientation, the misorientation or the grain boundary character. The data sets are further used to calculate the Schmid factors of the individual grains, and, as a statistical average of texture over the sampled specimen area, the orientation distribution function and the misorientation distribution function.

As a compliment to electron diffraction and conventional X-ray diffraction, an X-ray scanning apparatus has been developed for pole-figure measurement on selected small areas as well as for mapping the spatial distributions of crystal texture, residual lattice strain and element composition on bulk surfaces. The apparatus is based on energy dispersive X-ray diffraction. Spatial resolution of pole-figure measurement and residual lattice strain mapping is presently 0.1 mm, whilst resolution of texture and micro X-ray fluorescence element maps is about 0.05 mm. Residual lattice strain down to $\Delta a/a = 4 \cdot 10^{-4}$ is analyzed by evaluating the shifts and profiles of diffraction peaks in the spectrum.

1. INTRODUCTION

Natural (e.g., minerals, rocks, metals, or bones) as well as man-made materials (e.g., metals, ceramics, crystalline polymers) are often assumed

*) present e-mails: mail@ebsd.info   post@robert-schwarzer.de
web: www.ebsd.info   www.crystaltexture.com

to behave equally in all directions, although most of them have an individual polycrystalline structure. The anisotropy of the individual crystals, however, is only balanced out in case of a large number of grains *and* a random distribution of the grain orientations. In reality, a residual anisotropy is found which varies, depending on the actual statistical distribution of grain orientations—the "crystal texture", "preferred crystal lattice orientations"—between the extreme values of the anisotropic physical property in the single crystal. Hence, texture is of major scientific interest as well as of great importance in a wide range of industrial applications.

Noticeable advances in texture analysis [cf.[1,2] and references therein] have been made recently by the development of automated X-ray texture goniometers including position sensitive, two-dimensional, CCD and energy dispersive detectors, and by the introduction of new X-ray optics. *Local* variations in *crystal texture* may give rise to *inhomogeneous material properties* which may finally limit the performance of a workpiece. Therefore, the measurement of local texture and its graphical representation are of great concern for quality control and basic research. As a supplement to the established techniques of global texture measurement by X-ray, synchrotron radiation and neutron diffraction, approaches have been made for the study of preferred crystal lattice orientations on a grain-specific scale with computer-controlled electron microscopes. These electron diffraction techniques have reached a high stage of development[2]:

- Pole figures of small areas are obtained from thin foils in SAD or from bulk surfaces in RHEED mode of the TEM,
- Automated Crystal Orientation Measurement/Mapping (ACOM) grain by grain by interpreting Kikuchi patterns in the SEM or TEM is about to become a mainstay of modern microstructure analysis.

2. ON-LINE MEASUREMENT OF POLE FIGURES WITH THE TEM

Selected Area electron Diffraction (SAD) in the TEM is the conventional technique to study the crystal structure of thin films at a high spatial resolution, The distributions of intensity along the diffraction rings are a quantitative measure of the volume fraction of grains with preferred orientations related to the particular diffraction vectors (pole densities). If there is, for instance, a polycrystal with preferred crystal lattice orientations about one axial direction (fibre texture), texture patterns are

obtained with sickle-shaped peaks on the ring positions at oblique incidence of the beam and closed rings when the fibre axis is oriented parallel with the beam, SAD pole-figure measurement[2] is based on this feature: The specimen is placed in the side-entry goniometer of the TEM in such a manner that a reference direction (e.g., the rolling direction) is parallel with the goniometer axis. The specimen area of interest is first inspected in imaging mode. Then the microscope is switched to selected area diffraction. A series of diffraction patterns have to be considered for texture analysis. Hence, diffracted intensities are measured on chosen ring positions while tilting the specimen in small incremental steps through large angles about the goniometer axis. The tilt angle and the azimuth angle of a peak on the selected hkl diffraction ring define one point ("pole") on the hkl pole figure.

Automated intensity measurement is carried out by deflecting, under computer control, either the whole diffraction pattern past the objective lens on a circle along a selected diffraction ring (Figure la), or by deflecting the primary beam before the objective lens along a cone with semi-apex angle $2 \cdot \theta$ (Figure 1b). The diffracted intensities are measured either in diffraction mode with a Faraday cup, or—only possible in the case of conical pre-specimen deflection—in imaging mode of the TEM by taking the intensities from the dark field images. Speed and accuracy of on-line pole-figure measurement with the TEM has been improved significantly by replacing the serial measurement of intensity by a parallel acquisition of the whole diffraction patterns or dark-field images, respectively. An integrating high-resolution CCD camera is used as an area detector. The diffracted and the background intensities are then extracted pixel by pixel along the diffraction rings with the computer. From the dark-field images, however, the positions and orientations of the individual grains can be extracted in conical pre-lens deflection mode. They can be used in a refined analysis of orientation stereology,

Textures of thin surface films on bulk substrates are measured with a RHEED (Reflection High-Energy Electron Diffraction) setup in the TEM (Fig. 1c)[2]. The specimen is mounted on a special holder close to grazing incidence of the primary beam. It is rotated under computer control in incremental small steps about its surface normal while the RHEED texture patterns are picked up at each step with the CCD camera and passed to the computer for extracting the diffracted intensity values. Almost complete pole figures are thus obtained within a few minutes. The primary beam may be scanned in a line across the specimen to widen the sampled specimen area from a small vertical strip to a rectangle such that the whole specimen surface is immersed in the beam. As in backscatter XRD, the surrounding material may be removed or masked by careful preparation. Spatial resolution of RHEED pole-figure measurement ranges
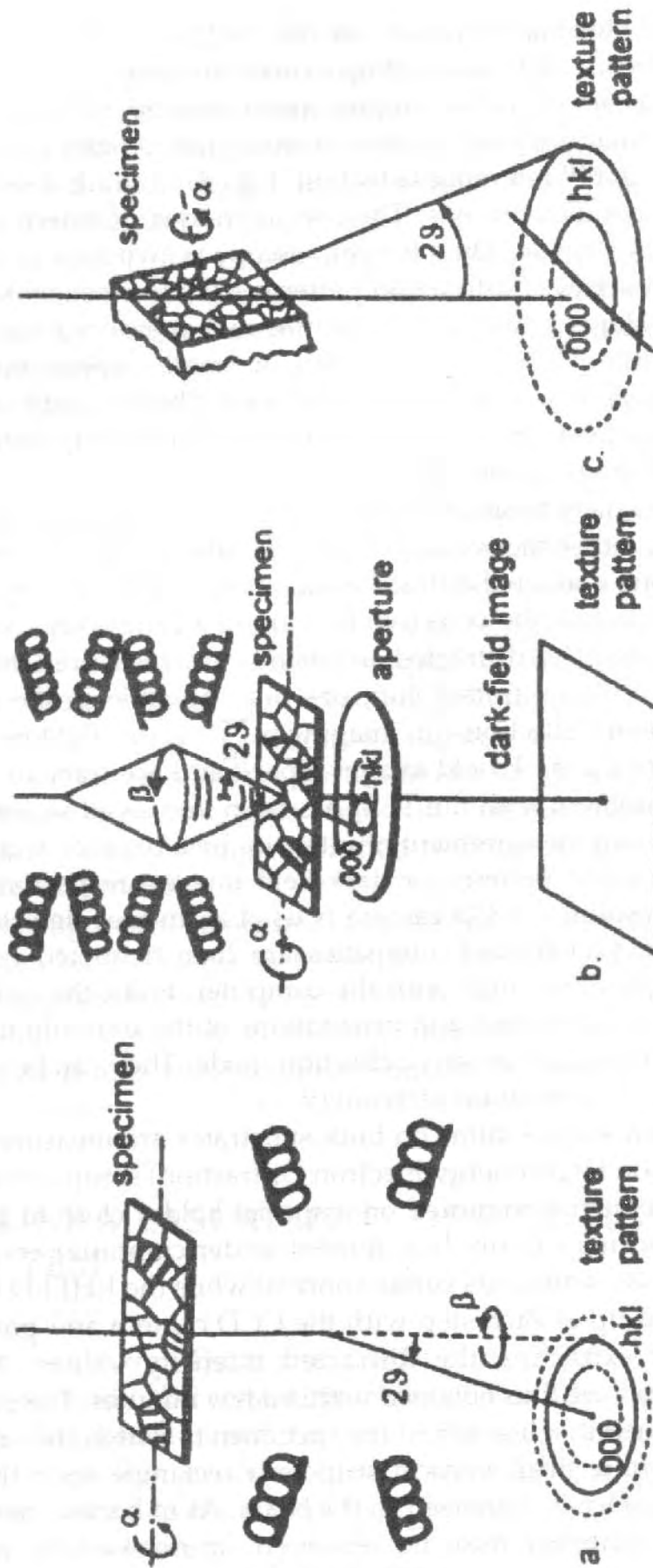
Figure 1: The acquisition of pole figures in the TEM.
a. Circular post-lens deflection b. Conical pre-lens deflecten c. RHEED setup

from less than a tenth to several millimetres. The benefits over grazing incidence X-ray pole-figure measurement are an extreme surface sensitivity and a high speed.

Pole figures can be measured in transmission down to almost the smallest specimen regions defined by selected area diffraction (0,5 µm diameter). Applications of this technique have been the study of deformation texture of shear bands and deformation bands in cubic and hexagonal materials. Two correction procedures have been developed to interpret quantitatively the diffracted intensities in terms of pole-to-volume distribution. The Orientation Distribution Function (ODF) of small areas can be calculated from experimental TEM pole figures using inversion methods similar as in standard X-ray texture analysis.

3. INDIVIDUAL GRAIN ORIENTATION MEASUREMENT

3.1 TRANSMISSION ELECTRON DIFFRACTION

SAD spot patterns, when applied to precise crystal lattice orientation measurement, lack from the limited definition of the sampled specimen area (no better than about 0,5 µm, mainly due to the spherical aberration of the objective lens), from a low accuracy of experimental orientation data (as a result of the spiking of reciprocal lattice points in directions of small crystal dimension; typical errors are about *5°,* unless tedious techniques are employed) and from the susceptibility to ambiguous indexing since a spot pattern is usually made up of spots of one common zone axis only. Electron diffraction spot patterns are, however, still required for orientation measurements with very thin specimens, after heavy deformation, for studying small grains or orientation relationships between the matrix and small precipitates.

Convergent Beam Electron Diffraction (CBED) is sometimes used as an alternative technique for obtaining a high spatial resolution with older TEM. CBED suffers from the excessive widening of the diffraction spots when the beam diameter is decreased for focusing on the grain of interest. The patterns are, therefore, of very limited use for crystal lattice orientation measurement. CBED patterns are used on a grain-specific level either for the determination of local foil thickness and structure potentials of the crystal lattice, or for the determination of crystal lattice symmetry (space and point group), for phase identification, for the characterization of stacking faults and Burgers vectors and for residual strain measurement.

Transmission Kikuchi Patterns (TKP) are formed in the TEM instead of spot diffraction patterns, if the diffracting volume is an almost perfect

and sufficiently thick crystal to scatter some portion of the primary electrons inelastically through large angles. Film thickness may range from the mean free path length of the primary beam electrons to some micrometres, depending on the accelerating voltage and density of the particular material. The possibility to use thick specimens in the TEM is a major advantage of Kikuchi diffraction. Thin foils, suitable for spot or CBED patterns, are often difficult to prepare and may hardly be representative for the bulk material. In addition, local foil bending is reduced significantly with increasing thickness and will so less affect accuracy of measured orientation data. The beam convergence is not relevant for the formation of a Kikuchi pattern, as inelastic scattering will spread the primary beam into all directions, that is over a much larger angular range than can ever be obtained by means of focusing an electron lens on the specimen at a short distance. Hence, the term CBED is not appropriate for Kikuchi diffraction with regard to local orientation measurement, although Kikuchi lines are also present in CBED patterns. Kikuchi patterns in Micro Beam electron Diffraction (MBD) enable more reliable orientation measurements than spot patterns do. This can easily be verified by watching the diffraction pattern from a single crystal of medium thickness, which may then contain some diffraction spots and Kikuchi lines at the same time. When tilting the specimen through a few degrees, the Kikuchi lines rigidly and precisely follow every rotary movement of the crystal, whilst the diffraction spots may only change their intensities rather than their positions with respect to the primary beam spot. In practical work, the smallest probe size and hence spatial resolution is limited to about 10 nm with TKP, due to the decrease in image brightness as the probe becomes smaller, and due to the spread of the scattered beam on its way through the specimen foil. If neighbouring grains are studied, orientation differences down to 0.1° can be measured. When evaluating the crystal lattice orientation with respect to the workpiece, additional errors may be introduced by misalignments of the sample and the microscope. An outstanding feature of the TEM is the ability to produce a high-resolution image and alternatively, a diffraction pattern of the same selected area by simply switching from imaging to diffraction mode of operation.

3.2 BACKSCATTER ELECTRON DIFFRACTION

Add-on facilities for generating Electron Channeling Patterns (ECP) from selected small specimen regions are still available with some commercial SEM. Since spatial resolution is hardly less than 50 µm, as a consequence of the pivoting beam, ECP have been superseded for most applications in materials science by backscatter and transmission Kikuchi patterns during the last decade.

Backscatter Kikuchi Patterns (BKP)[3,4] are generated by back-diffraction of a stationary beam of high-energy electrons from an almost perfect volume of crystal. The characteristic feature of a BKP is the regular arrangement of straight bright bands—rather than diffraction spots as in SAD—on a steep continuous background which intersect in "star-like" zones. The geometry of a Kikuchi pattern can be interpreted as a gnomonic projection of the crystal lattice on a flat fluorescence screen. The point of impingement of the primary beam on the specimen surface is the centre of projection. In particular, the angles between the centre lines of the Kikuchi bands correspond to interplanar angles, and the widths of Kikuchi bands correspond, according to Bragg's law, to interplanar spacings. The "stars" correspond to zone axes of the crystal. The extinction rules due to the structure factor of the crystal lattice apply for expected reflections, and high order reflections may appear as a set of straight lines parallel with the band edges. The intensity distribution in a Kikuchi pattern is not explained by this simple geometric model, but the dynamic theory of electron diffraction has to be employed. For crystal orientation measurement, however, the geometry of band width and band position as mentioned above is sufficient. Backscatter Kikuchi patterns, when acquired in the SEM with a video camera have also been named Electron Back Scattering Patterns (EBSP)[5], and this acronym is now frequently used in particular with commercial systems for orientation measurement.

In the SEM, the bulk specimen has to be steeply tilted to typically 20° to 30° from grazing incidence (Figure 2)[6], in order to obtain sufficient BKP intensity. The maximum of pattern intensity is close to optical reflection, because of the strong forward scattering of high-energy electrons. For acquisition, either a photographic plate or a transmission phosphor screen is placed parallel with the incident beam, right in front of the tilted specimen. A pattern covers a wide angular range up to ±60° and contains several principal zone axes. In a RHEED setup the specimen surface is inclined only a few degree from grazing incidence. It is then more convenient for recording the BKP to place the screen or photographic plates beneath the specimen at a right angle to the primary beam.

The steep specimen tilt is a drawback of Backscatter Kikuchi Diffraction (BKD) since the beam spot on the specimen as well as the orientation maps and conventional SEM images, when taken at the same specimen tilt, are heavily foreshortened. Spatial as well as depth resolutions in BKD depend on specimen tilt, density of the specimen and accelerating voltage. With our system, the lowest practical beam voltage is 3.5 kV using a tungsten filament. Spatial resolution with copper is significantly better than 0.1 μm at 20 kV. BKP have been found to disappear when a thin foreign surface layer is present of about two times in thickness as the Rutherford elastic mean free path is at a given beam
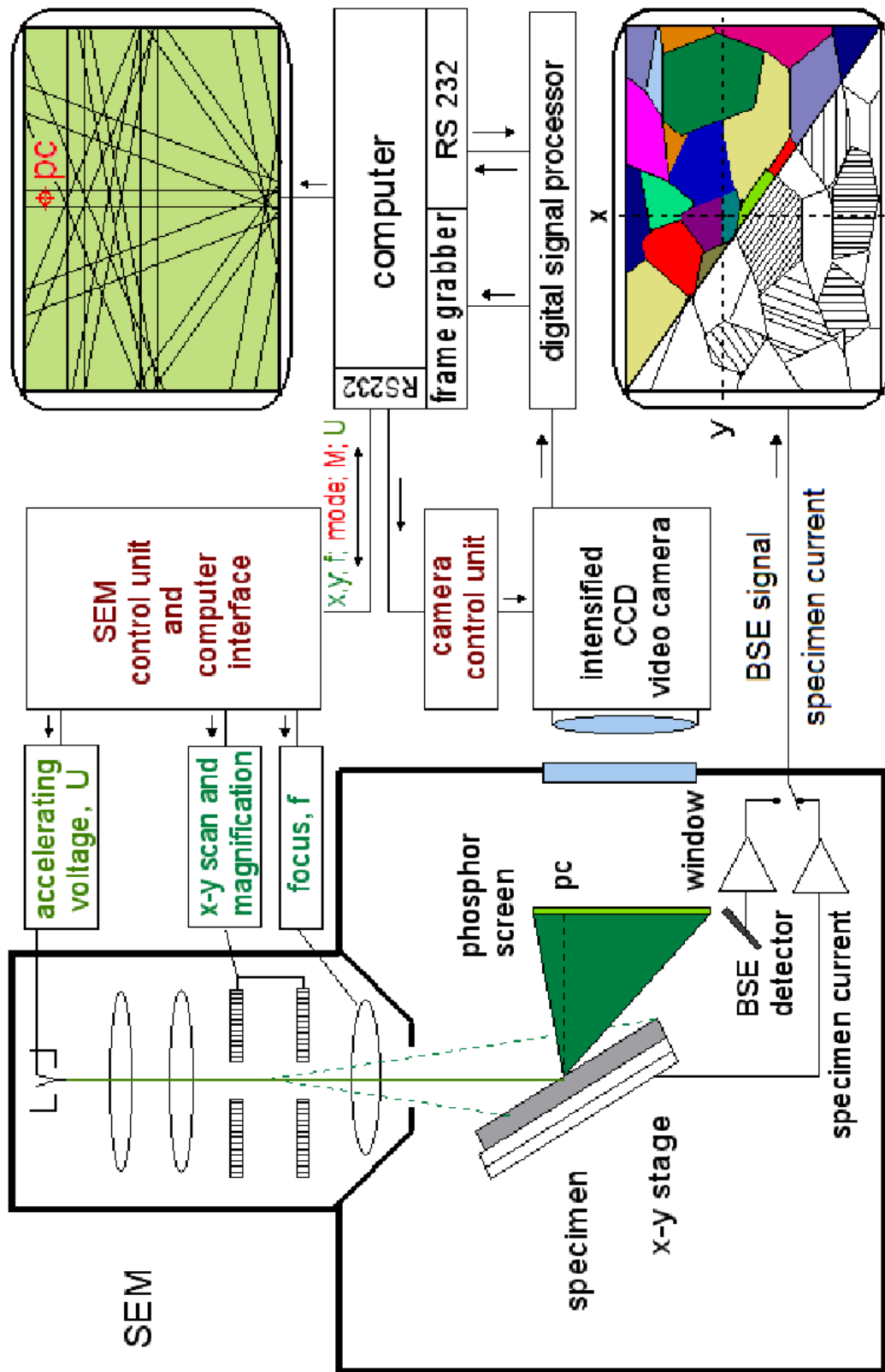
Figur 2: Experimental setup for automated cryslal orientation measurement with a computer-controlled SEM by interpreting backscatter Kikuchi patterns.

energy, i.e. a depth resolution is assumed of about 100 nm for Al, 20 nm for Ni and 10 nm for Au at 40 kV accelerating voltage and 20° angle of incidence.[7]

The accuracy of orientation measurement with the SEM is limited to about 1° to 2°. This is often sufficient for analyzing crystal texture. A detailed study of misorientations or the distribution of special grain boundaries, however, might require a higher precision of the individual lattice orientation data. Then the transmission Kikuchi technique in the TEM or micro-Kossel X-ray diffraction are superior.

3.3 ON-LINE ACQUISITION AND INTERPRETATION OF KIKUCHI PATTERNS

Crystal lattice orientations can be determined with high precision from Kikuchi and channeling patterns since the lines, respectively the band edges, are sharp and exactly follow any rotation or tilt movement of the crystal. It is, hence, sufficient to simply measure the *positions* of Kikuchi bands or zone axes in the pattern. With spot diffraction patterns, however, the *diffracted intensities* have to be considered in addition to obtain a reliable indexing of the beam direction.

The same methods can be used for indexing transmission and backscatter Kikuchi as well as channeling patterns since their geometry is quite similar. Indexing is unambiguous if the positions of three bands are available which do not have a zone axis in common. Taking into account unavoidable inaccuracies in the measured beam positions, a much larger number of 8 or more consistently indexed bands is recommended, in particular to exclude false orientation values with low-symmetry crystal lattices. In the TEM the built-in beam deflection coils may be used for extracting the band positions. An alternative technique in the TEM and the older set-up for backscatter Kikuchi patterns in the SEM is to acquire the diffraction patterns either directly with a CCD camera in the microscope or from a phosphor screen with a high-gain TV camera through a window from outside. The digitized patterns are then processed with a computer to reduce background. Finally, the operator marks the positions of bands or zone axes with the cursor on the monitor screen, and indexing is performed on-line using adequate software.

A great number of individual grain orientations are required for quantitative texture analysis. Therefore, the interactive collection of a significant database by the operator is inconvenient. Fully automated methods have been developed for acquisition and indexing of Kikuchi patterns with the SEM[8, 9] and the TEM[10] without the interaction of an operator. The band positions are extracted from the pattern by applying a modified Hough or a Radon transform. Orientations are measured at spatially specific points by a digital scan of the electron beam across the

specimen surface and automated interpretation of the backscatter Kikuchi patterns (ACOM). A computer-controlled, high precision *x-y* stage is a slow and expensive alternative for digital beam scan. In addition, it is susceptible to mechanical play and does hardly accommodate dynamic experiments neither at high temperatures nor *in situ* tensile tests. The advantages of a mechanical specimen scan is a large travel and the usability of much simpler indexing programs since the diffraction geometry does not change from one measured point to the next.

A modern ACOM software[6] has to control the mode of microscope operation (switching between imaging and spot/diffraction mode), the digital beam scan, final lens current settings (dynamic focus), magnification, accelerating voltage, and pattern acquisition (Figure 2). Dynamic calibration of the system is mandatory in particular for automated measurement at low magnifications. As a consequence of the steep specimen tilt in the SEM the working distance (lens focus), screen-to-spot distance (camera length) and the pattern centre (which marks one of the reference directions) vary with the spot position on the specimen surface during digital beam scan. Dynamic focusing of the probe-forming lens by the software is indispensable in particular with fine grain materials since a small probe size has to be guaranteed all over the measured area and at all magnifications. Dynamic focusing and autocalibration are not required with the TEM.

A high speed of more than 25,000 measured orientations per hour is presently achieved in the SEM. Speed is increased further by improved strategies of measurement. If, for instance, intragranular structure is of no concern, it is in principle sufficient to acquire the orientation of each grain only once. By iterative mesh refinement, measurement can be concentrated on grain boundaries. Speed is not only a virtue by itself in that the cycling time of the microscope is improved, but is indispensable for dynamic experiments (e.g., *in situ* hot stage, tensile or bending test experiments).

3.4 INTERPRETATION AND GRAPHICAL REPRESENTATION OF GRAIN ORIENTATION DATA

The orientation database from ACOM can be used for a statistical description of texture by constructing pole figures or calculating the ODF. In bulk workpieces, a high (statistical) sample symmetry of preferred orientations is often found that reflects the symmetry of the production process. Local texture, however, may have lower sample symmetry. Therefore, a supplementary program, based on the series expansion method, has been developed[11] which enables the calculation of the ODF, the MisOrientation Distribution Function (MODF), Orientation Correlation Functions (OCF) and derived quantities for all sample and crystal

symmetries from ACOM as well as from pole-figure data. Crystal lattice orientation measurement grain by grain yields information on the microstructure that is not obtained by any other technique. In particular, the study of correlations between spatial and orientation parameters is enabled. At each point of the scan grid, the x-y coordinates are recorded that describe the position, along with three Euler angles describing the local grain orientation, the pattern quality and a confidence level describing the local lattice strain. The blur of a pattern is a measure of local dislocation density. Misorientations Δg across grain boundaries are directly available from ACOM. As a further characteristics the *crystallographic direction* of the grain boundary normal **n** is determined by measuring the *spatial inclination* of the grain boundary plane, e.g. by tilt experiments in the TEM or by serial sectioning with the SEM. The amazing result for $\Sigma 3$ twins in annealed nickel sheet metal[12] is that about half of the boundaries were asymmetrical twist boundaries on the 110 zone, and correlate with proximity to the 111/111 symmetrical tilt boundaries. In polysilicon, only 40% of the $\Sigma 3$ boundaries were close to 111/111 twins and 20% close to 211/211 twins[13] which are supposed to show "special" properties. A particularly interesting application is the study of triple point geometry and the evaluation of grain boundary energies. With the TEM under computer control, structural features such as dislocation line directions can be indexed and Burgers vectors determined conveniently in addition to orientation measurement, thus enabling the rapid identification of deformation systems in low-symmetry crystals.[14]

The spatial distributions of grain orientation are visualized by assigning orientation-specific pseudo-colours to the measured points on the scanning grid to construct Crystal Orientation Maps (COM) or "orientation images" of the microstructure (Figure 3). In a similar way, misorientations across grain boundaries, Σ values of grain boundaries, or other microstructural characteristics and derived entities such as dislocation densities, activated glide systems, types of twins or resolved shear stress are visualized by staining the grains in the micrograph with specific colours.[14] All grain boundaries exceeding some tenth of a degree are identified. Orientation contrast in conventional microscopy, on the other hand, relies on various mechanisms of contrast formation which are related to lattice orientation gradients, but in rather complex ways. Chemical etching of metallographic surfaces, for instance, is intended to produce an orientation-related surface relief. The mechanisms of etch attack, however, as a function of surface orientation, misorientation and degree of deformation of the disturbed boundary layer between grains are not known in detail. So the formation of image contrast is mainly based on practical experience. Certain boundaries or grains like twins may not be revealed reliably by metallographic methods. The statistical distribution of grain size, for instance, as determined in conventional microscopy is then apparently biased by the skill of the operator.

Figure 3: Crystal orientation maps of a Nickel specimen constructed from ACOM data.

Electron diffraction in general does not provide lattice constants from the Bragg equation with the same precision as X-ray diffraction to facilitate a straightforward phase analysis. Automated phase discrimination, however, is often possible from indexing and simulating Kikuchi patterns by a trial-and-error technique, provided that the lattices are sufficiently different by symmetry or lattice constants. If indexing is successful for only one crystal structure, other possible phases with different structures can be excluded (Figure 4). EDS analysis, on the other hand, cannot distinguish between phases of similar element composition. Phase identification has been carried out successfully by using a scientific grade slow-scan cooled CCD camera for the acquisition of high-quality BKP.[15] Phases of selected areas can be determined from symmetry considerations, simulation of Kikuchi pattern intensities and precise measurement of angles between zone axes. The most reliable and a high-resolution technique for phase identification in the TEM is the interpretation of zone-axis patterns in CBED.

The benefits of analytical electron microscopy are the correlation of morphology (from the micrograph) and element composition (from EDS analysis) with crystal lattice orientation and phase (from ACOM) on a submicron scale. Therefore, ACOM will enable a major progress in stereological interpretation of microstructure. The number fraction of array points assigned by measurement to a specific property (e.g., crystal orientation or lattice strain) can directly be equated to the area fractions of grains having this considered property.
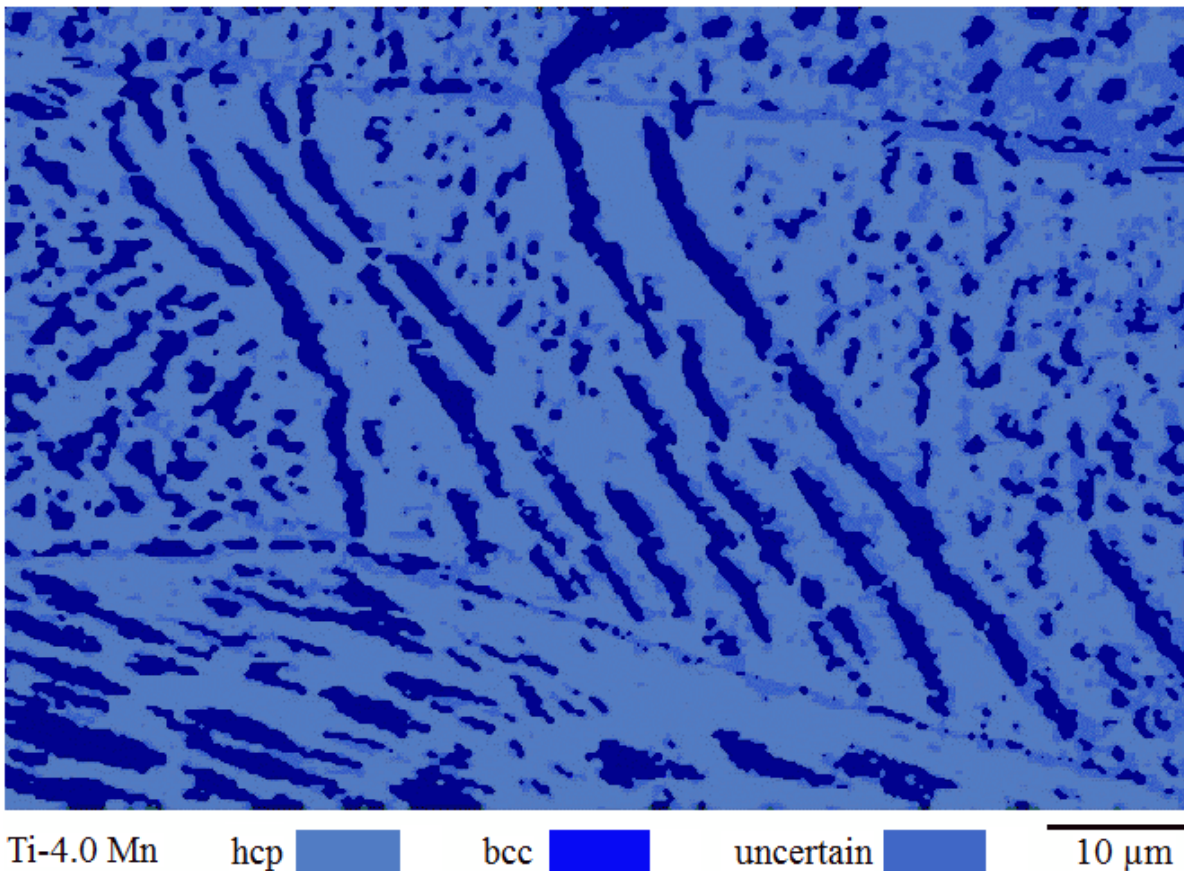
Figure 4: Phase distribution map of a dual-phase Ti-4.0 Mn specimen. Phase discrimination has been performed by ACOM in the SEM without the interaction of the operator.

3.5 EXAMPLE OF APPLICATION OF ACOM

Continuous thin metal layers, deposited on a solid substrate by sputtering or evaporation under high vacuum or by electroplating, often exhibit a marked fibre texture. Grain structure is increasingly becoming important when the dimensions of the layers are in the range of average grain size. This is, in particular, the case with interconnect lines in modern microelectronic circuits. Copper, due to its high electromigration resistance, is one promising candidate to replace aluminum as the standard metallization material, although some difficulties in line structuring, corrosion resistance and incompatibility with the semiconducting base material have not yet been overcome. Copper layers are usually electroplated into narrow damascene trenches to achieve extremely narrow lines with sharp edges. Thus, they are subjected to geometric constraints on grain growth by the trench sidewalls and the bottom during deposition and recrystallization.

In this example[16] about 1 µm thick copper layers have been electroplated into trench-structured SiO_2/Si substrates for further investigations of reliability and electromigration resistivity. The trenches were 1.0 µm wide, 0.5 µm deep and PVD coated with 50 µm tantalum as a barrier layer. In addition, a PVD copper seed layer has been deposited at 50 °C. After the electroplating process the wafers were annealed for ten minutes at 120 °C. Finally, the continuous copper layer has been removed by chemical-mechanical polishing (CMP) down to the damascene trenches.

In the crystal orientation maps (Figure 5), the crystal orientations are represented by pseudo-colours (or in gray tone) in every pixel element. All grains are clearly discriminated from each other, in contrast to conventional SEM images. A central seam of grain boundaries has been formed in several interconnect lines which is supposed to result from grain growth from the trench walls, in addition to grain growth from the bottom. The competing directions of grain growth are supposed to give evidence in texture. Therefore, the ODF and pole figures have been calculated with the series expansion method[11] from the measured crystal orientations, separately for those grains which fill an interconnect line at full width (bamboo grains) and for those grains which form the central seam. Preferred <111> and <115> orientations have been found, indeed, for both types of grain with their fibre axes aligned perpendicular either to the specimen normal direction or to the trench walls, respectively.
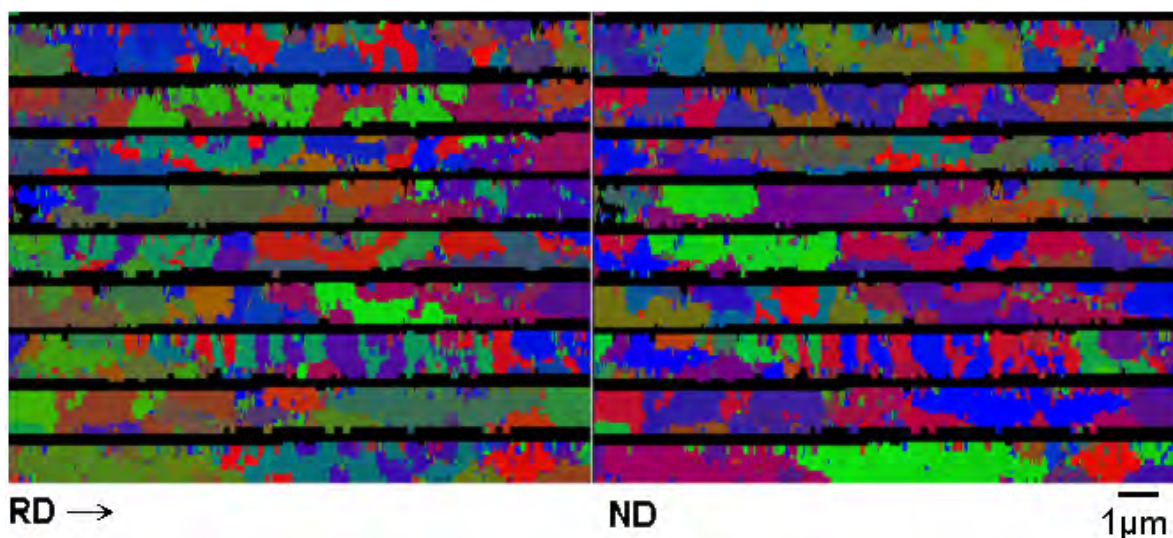

Figure 5: Crystal orientation map of a damascene copper interconnect line.
The crystallographic grain directions {hkl} and <uvw> oriented parallel with the specimen normal ND (right map) and the in-plane reference direction RD (left map) are encoded in pseudo-colours.

4. MAPPING OF LATTICE STRAIN AND TEXTURE DISTRIBUTIONS BY X-RAY DIFFRACTION

4.1 THE X-RAY SCANNING APPARATUS

Electron diffraction in the SEM, though powerful, is not a universal technique to meet all requirements of local texture measurement. Some examples of limited application are excessive deformation, small grain sizes, or incompatibility of the specimen with vacuum or irradiation by electrons. Some other applications only require the knowledge of the spatial distributions of certain *crystal lattice directions* averaged over small areas (i.e. pole densities) in the specimen surface or cross-sections rather than the full *crystal lattice orientation* of each grain. Spatial resolution of conventional X-ray pole-figure measurement on the other hand, is often insufficient for studying texture gradients or local texture.

To avoid some of these limitations, an X-ray Scanning Apparatus (XSA), based on Energy Dispersive (ED) X-ray diffraction, has been developed for "imaging" the spatial distributions of crystal texture, residual lattice strain, and element composition in bulk specimens as well as for pole-figure measurement on selected small areas.[17, 18] Spatial resolution is primarily dependent on the size of the X-ray spot and its elliptical elongation by projection on the tilted surface. A practical limit is presently at 0.1 mm for pole-figure measurement and lattice strain mapping and 0.05 mm for texture and micro X-ray fluorescence element mapping, because of the low intensity of the collimated primary beam. The system is based on a commercial two-circle goniometer and an open Euler cradle (PHILIPS X'Pert MRD goniometer). Mapping is performed by translating the specimen with a stepping-motor driven *x-y* stage step by step across a field up to 100 mm by 100 mm wide in a user defined mesh grid. Pole figures are measured by tilting and rotating the specimen in the Euler cradle through an equal step, equal area, thinned or incomplete user-defined angular grid (α, β) on the pole sphere.

4.2 ENERGY DISPERSIVE X-RAY DIFFRACTION

An ED detector is used for X-ray diffraction to enable the fast acquisition of a spectrum of several diffraction peaks at a time as well as the deconvolution of overlapping peaks and peak profile analysis. Standard solid-state ED Systems, as known from elemental analysis with the SEM, are well suited. The advantages over a position sensitive detector are for texture mapping:

- A high efficiency is obtained since non-filtered (white) primary beam radiation is used and almost 100% of the intensity falling on the detector is acquired.
- A very high count rate in the linear range is achieved.
- All diffraction peaks are related to the *same direction* in the specimen-fixed coordinate system, i.e. they represent the same point (α, β) on the pole spheres.
- X-ray fluorescence peaks may be evaluated for element analysis, in addition to diffraction peaks.
- Peltier cooled ED detectors, in particular those with a pin-diode, are compact and lightweight which accommodates a flexible setup of the goniometer system.

ED X-ray diffraction is based on Bragg diffraction of a collimated "white" primary x-ray beam

$$E_{hkl} = n \cdot h \cdot c / (2 \cdot d_{hkl} \cdot \sin \theta_{hkl}) \tag{1}$$

in dependence of the orientation distribution of the grains in the surface (Figure 6). (E_{hkl} stands for the photon energy of an (hkl) diffraction peak, n is the order of diffraction, h Planck's constant, c the velocity of light, and θ_{hkl} the Bragg angle for lattice planes of spacing d_{hkl}.) The spectrum of secondary X-rays is composed of broad diffraction peaks and sharp characteristic fluorescence lines superimposed by a low background of scattered primary radiation. Soft X-rays, however, are absorbed in air on the way to the detector such that micro X-ray fluorescence analysis of light elements is not enabled. Windows are placed on the centre of selected hkl diffraction peaks or fluorescence lines. For a graphical representation of the microstructure, the count rates falling in a selected window are represented pixel by pixel by pseudo-colors or by a gray scale to finally fill in maps of spatial texture distribution, of pole-density (hkl; α, β), or of element composition.

Figure 7 shows ED diffraction spectra from a deformed aluminum specimen at two different pole-figure points. The variations of individual peak intensities are clearly visible. A set of diffraction peaks can be identified. The low index peaks are all separated in the spectrum and no peak overlap occurs for 111, 200, 220 and 400. Characteristic fluorescence lines from aluminum are not present since soft X-ray radiation is absorbed in air on the path to the detector. *W* marks peaks of scattered characteristic tungsten radiation from the tube.

Lattice strain is analyzed and mapped, in addition to texture, with the same setup by evaluating the shift and width of diffraction peaks in the spectrum of each image point. The peak positions θ_{hkl} are compared with the peak position θ_0 from a relaxed specimen with lattice spacing
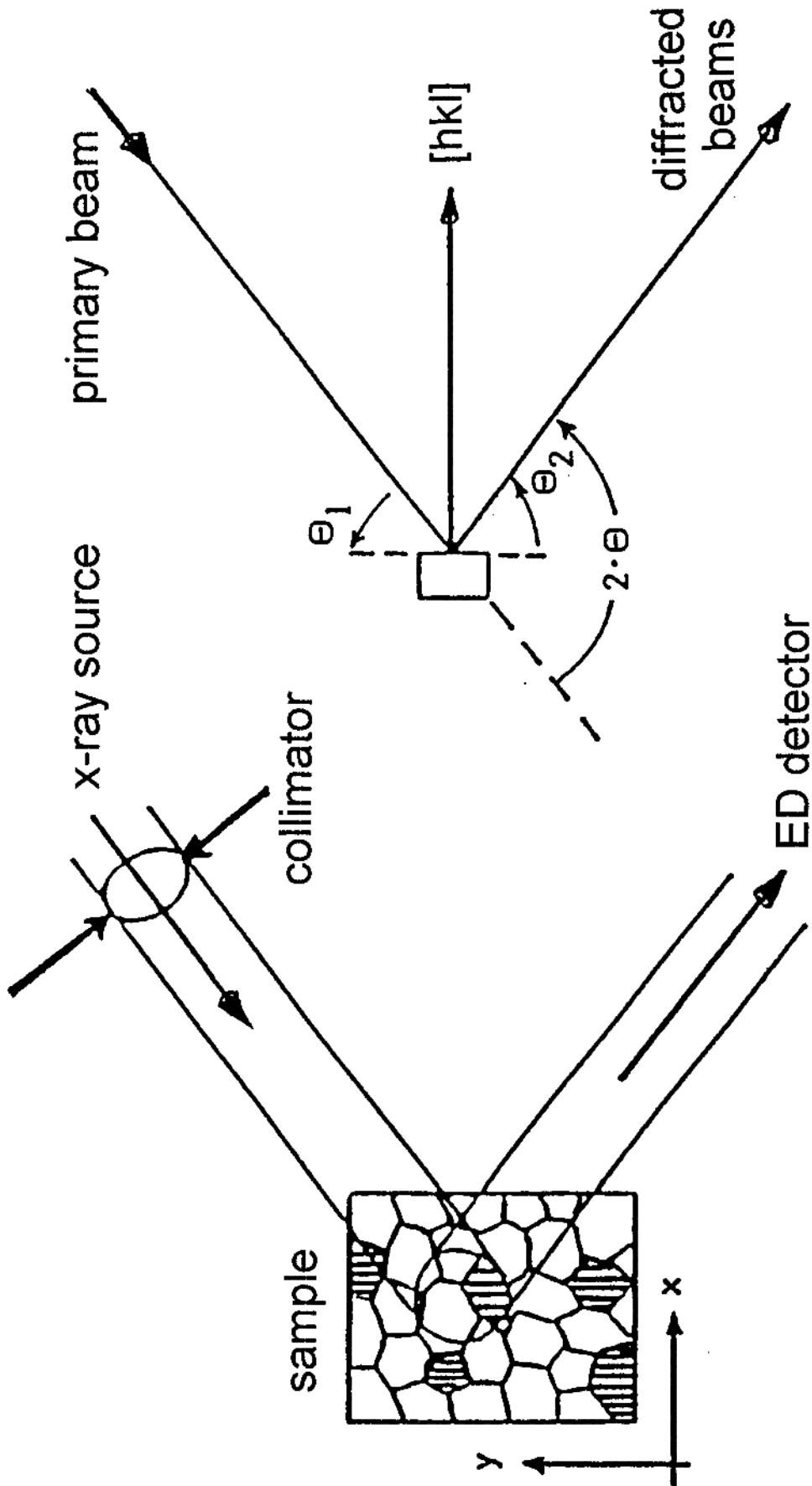
Fig. 6: The schematics of the X-ray scanning apparatus for the measurement of texture, residual lattice strain and element distribution (micro X-ray fluorescence analysis)
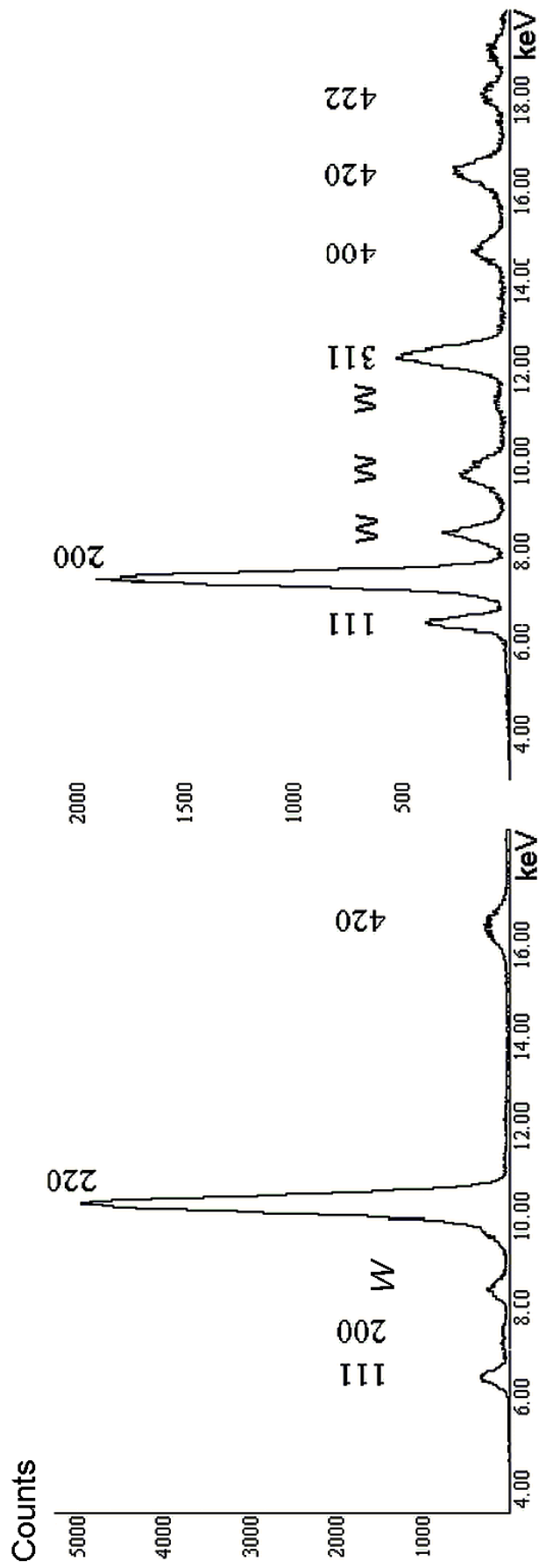
Figure 7: ED diffraction spectra from a deformed aluminum specimen. A tungsten tube has been used to generate a „white" primary X-ray beam.

d_0. The peak shifts, $\Delta\theta$, are a measure of long-range residual strain/stress of the first kind. From Bragg's equation follows

$$\Delta\theta = \theta_{hkl} - \theta_0 = - \tan\theta_0 \cdot (d_{hkl} - d_0)/d_0 \qquad (2)$$

or transformed to the scale of photon energy, E, which is more adequate for energy dispersive diffraction:

$$\Delta E_{hkl} = (E_{hkl} - E_0)/E_0 = (d_{hkl} - d_0)/d_0 \qquad (2a)$$

Line profile analysis is performed by Gauss fitting after background correction. The width of a diffraction line reflects the variations of lattice spacing, Δd, respectively residual strain from grain to grain in the diffracting volume, strain gradients across grains or microstructural imperfections in the grains (residual stress of the second and third kind).

Peak broadening due to the finite primary beam and detector apertures, limited spectral resolution and small grain size have to be considered, as well. In the X-ray scanning apparatus, the sensitivity and resolution of residual strain measurement are finally limited by the spectral resolution of the solid-state spectrometer system. A standard Si(Li) detector is used here with a nominal spectral resolution of 140 eV at 8.4 keV (Mn Ka line).

Any specimen reference direction (α, β) can be mapped provided that pole density (i.e. diffracted intensity) is high enough—which, of course, depends on local texture. It is worth noting that texture as well as residual strain are probed exclusively for those grains which satisfy the Bragg condition for the chosen specimen-fixed reference direction, e.g. the specimen normal direction in case of the symmetric goniometer setup with the specimen in a non-tilt position. There is no information acquired on grains at other orientations. Therefore, pole-figure measurement has to precede texture mapping on the same specimen area in order to recognize significant texture components.

4.3 EXAMPLE OF APPLICATION

A cross-section of an aluminum rivet was polished flat by gentle-mechanical grinding and finishing. A final electrochemical polishing was applied in order to remove any mechanical damage introduced during preparation. Several pole figures have been acquired in steps along lines across the head and the bolt of the rivet to recognize relevant texture components for texture and lattice strain mapping. A strong fibre texture has been found in the bolt region (Figure 8). The 220 diffraction peak P ($\theta_1 = \theta_2 = 20.1°$, $E_{220} = 12.62$ keV; $\alpha = 35°$ and $\beta = 83°$) has been used for evaluating at the same time the spatial distributions of pole density (texture map) and strain (residual strain map). Dwell time has been extended over 4 min./pixel to yield a sufficient count statistics in view

Figure 8: Pole figures acquired across the rivet bolt. The polar specimen direction P ($\alpha = 35°$, $\beta = 83°$) has been used for texture and residual strain mapping (cf. Figure 9).

of the low intensity. 2,232 Image points at a step width of 120 µm have been acquired.

A clear inhomogeneity is revealed in the texture (Figure 9a) as well as in the strain maps (Figure 9b). Two almost parallel strips of high pole density run along the axis of the bolt with a slight shift to the right hand side. They are supposed to form a tube of about 1/3 of the bolt diameter in the three-dimensional rivet. The head of the rivet shows a much lower density of this pole. It is worth noting that it forms a butterfly-shaped minimum that might result from punching the head during production.

There is a gradient in compressive residual strain along the bolt to the head. A dish-shaped maximum of compressive strain (dark) is found in the head, which is related to the butterfly-shaped minimum in the 220 texture map. There is an increased compressive residual strain in the interior of the "texture tube" (dark) and a tensile strain (bright) to the bolt surface. Statistics has been improved by averaging the peak shifts along a section of the shaft. So the radial distribution of residual strain across the bolt is clearly seen in the graph line (Figure 9c).

5. CONCLUSIONS AND OUTLOOK

The past decade has seen some remarkable progress in spatially resolved texture analysis. There is no "one-size-fits-all" method, and the choice depends on the sampled grain structure as well as on the degree of information necessary for texture analysis. A comparison is given in Table 1.

The majority of individual grain orientation measurements has so far been performed by the backscatter Kikuchi pattern technique with the SEM. This is due to specific advantages of SEM over TEM. First, SEM are widely used in many laboratories and in addition, several commercial systems and computer programs for backscatter Kikuchi pattern analysis are available. The operation of an SEM is less sophisticated. The sample preparation is simple. Finally, dynamic heating or tensile stage experiments can be performed conveniently in the SEM. TEM investigations are indispensable with fine-grain materials, at higher degrees of local deformation, or when microstructural features have to be quantified such as Burgers vectors of dislocations and deformation systems. Local texture in extremely deformed or fine-grain materials can be studied by TEM pole-figure measurement.

The correlation of spatial and orientation parameters and the high speed of ACOM with the SEM will facilitate a 3D reconstruction of the microstructure of the bulk, e.g. with serial sectioning, by merging the two conventional but still separated branches of microstructure characterization that are quantitative stereology and texture analysis to a more general concept of (3D) orientation stereology.
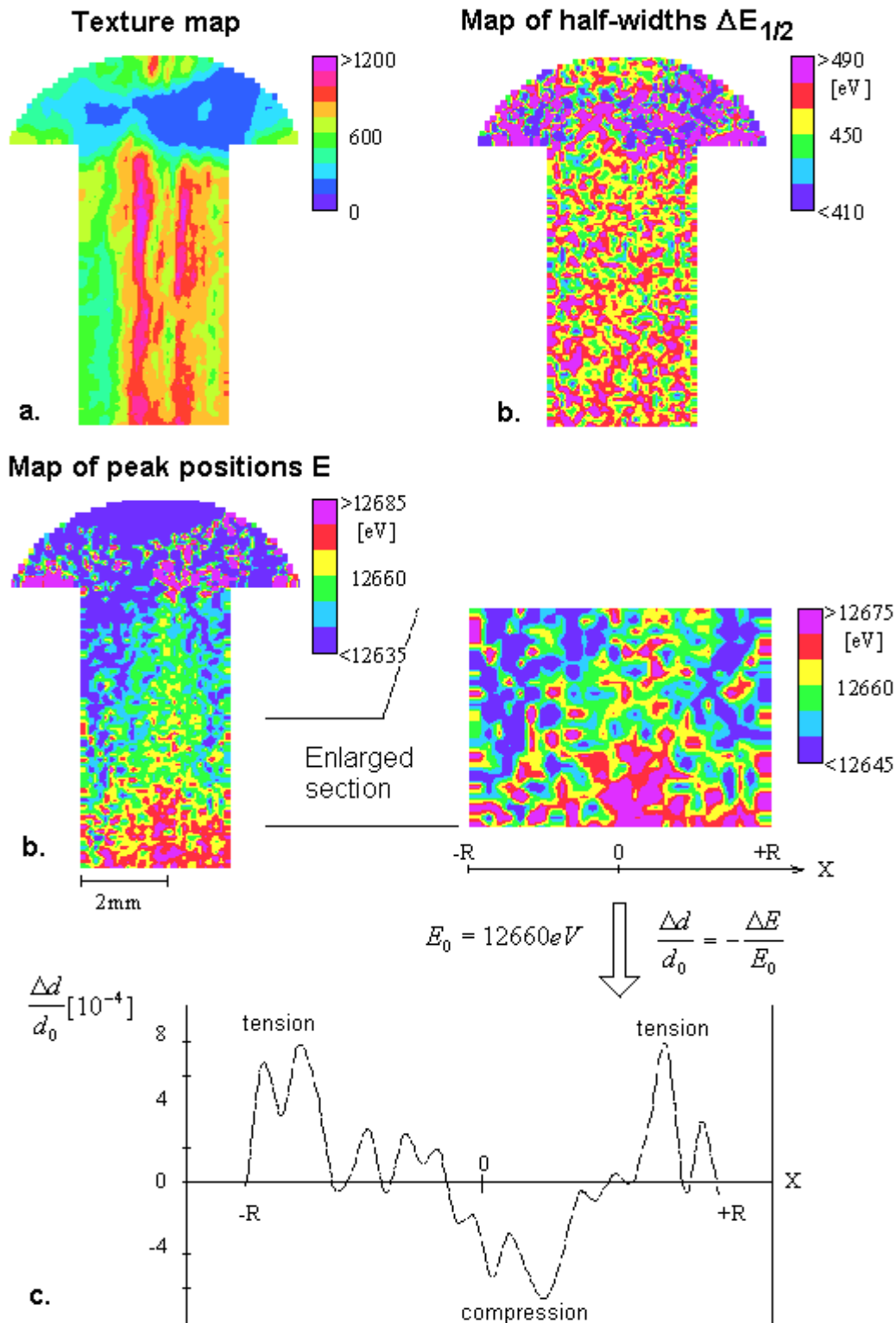
Figure 9: Cross-section of an aluminum rivet. Distribution maps (a) of the intensity (pole density, texture) and (b) of the shift (residual strain) of the 220 peak at pole P ($\alpha = 35°$, $\beta = 83°$). (c) The lattice strain $\Delta d/d$ across the bolt.

Table 1. Comparison of diffraction methods for measurement.

Type of pattern	Equipment	Resolution		Main applications
		spatial	angular	
Spot pattern	TEM (selected area diffraction = SAD)	0.5-1.5 µm	5° (1°)	thin foil specimens, dark field imaging, dislocations (weak beam) Burgers vector analysis, precipitates, nano-materials, orientation relationships, (estimate crystal orientations)
Transmission Kikuchi pattern (TKP)	TEM (SAD)	0.5-1.5 µm	0.2°	thick foil specimens, medium size grains, crystal orientations, orientation differences, dislocation density
	TEM (microbeam diffraction, = "MBD") STEM	10 nm	0.2°	thick foil specimens, fine grain structures, crystal orientations, ACOM, orientation differences, indexing of grain boundaries, deformed materials, grain growth
Backscatter Kikuchi pattern (BKP, "EBSP")	SEM with a BKP appliance (low light level (video) camera, computer control) several commercial ACOM systems available	0.05-1 µm	1°-2°	bulk specimens, coarse grains, mesostructure, crystal orientations, ACOM, dynamic experiments (e.g., hot stage, tensile stage), fracture surfaces, (residual stress) phase identification (phase ID)
(SAD) Channelling pattern	SEM (as an option for some SEM commercially available)	10 - 50 µm	0.5°	bulk samples, semiconductors (gentle method), crystal orientation, orientation differences, residual stress, fracture
TEM pole-figure measurement	TEM with a side-entry goniometer, video camera and/ or computer control	1 µm (SAD) 0.1 mm (RHEED)		thin film specimens (SAD) bulk surfaces, layers (RHEED), very fine grain structures, high degree of deformation, shear bands, texture fields
X-ray diffraction X-ray scanning apparatus	Euler cradle, with x-y stage and ED detector	0.1 mm 50 µm 0.1 µm		local pole figures, texture mapping, element mapping (micro XRFA), lattice strain mapping

A technique complementary to Standard X-ray pole-figure measurement and electron diffraction is available with an X-ray scanning apparatus based on energy dispersive diffraction. It enables spatial distribution maps of crystal texture, element composition and local lattice strain related to the same specimen area up to several cm^2 wide. The gentle technique is well suited for conductive, recrystallized and flat bulks as well as delicate, non-conductive, deformed, fine-grain and rough specimens. Spatial resolution is 0.1 mm or better in pole-figure measurement and mapping.

6. ACKNOWLEDGEMENT

REFERENCES

[1] H.J. Bunge and C. Esling: *Texture et Anisotropie des Matériaux,* Techniques de l'Ingenieur, Traité Materiaux Métalliques M **605**, pp. 1, Paris (1998).

[2] R.A. Schwarzer, *Mat. Sci. Forum,* **287-288**, 23 (1998).

[3] Sh. Nishikawa, and S.Kikuchi: *Proc. Imp. Acad. Japan* **4**, 475 (1928).

[4] M.N. Alam, M. Blackman, and D.W. Pashley: *Proc. Roy. Soc.* **221***,* 224 (1954).

[5] J.A. Venables, and C.J. Harland: *Phil. Mag.* **27**, 1193 (1973).

[6] R.A. Schwarzer: *Micron* **28**, 249 (1997).

[7] J.R. Michael, and R.P. Goehner: Proc. 52nd Annual Meeting MSA, pp. 596 (1994).

[8] N.C. Krieger Lassen, D. Juul Jensen, and K. Conradsen: *Scanning Microscopy* **6**, 115 (1992).

[9] B.L. Adams, S.I. Wright, and K. Kunze: *Met. Trans.* **24a**, 819 (1993).

[10] S. Zaefferer, and R.A. Schwarzer: *Z. Metallkunde* **85**, 585 (1994a).

[11] B. Schäfer : *Mat. Sci. Forum* **273/275**, 113 (1998).

[12] V. Randle: *J. Mater, Sci.* **30**, 3983 (1995).

[13] F. Wagner, P. Obringer, R.A. Schwarzer, G. Goaer, and D. Sarti: Proc. 11th Intern. Conf. Textures of Materials (ICOTOM-11), Xi'an (China), pp. 1406-1409, (1996).

[14] R.A. Schwarzer : *Ultramicroscopy* **67**, 19 (1997).

[15] J.R. Michael, and R.P. Goehner: *MSA Bulletin* **23**, 168 (1993).

[16] A. Huot, A.H. Fischer, A. von Glasow, and R.A. Schwarzer: Proc. 5th Intern. Workshop on Stress-Induced Phenomena in Metallization, AIP Conf. Proc. **491**, Melville New York (1999), pp. 261-264

[17] A.H. Fischer, and R.A. Schwarzer: *Mater. Sci. Forum* **273-275**, 255 (1998).

[18] A.H. Fischer, and R.A. Schwarzer: *Mater. Sci. Forum* **273-275***,* 673 (1998).

ACRONYMS USED IN THIS ARTICLE

ACOM	Automated Crystal lattice Orientation Mapping/Measurement
BKD	BackScatter Kikuchi Diffraction
BKP	BackScatter Kikuchi diffraction Pattern
CBED	Convergent Beam Electron Diffraction
COM	Crystal Orientation Map
EBSD	Electron BackScatter Diffraction (= BKD, ACOM with the SEM)
EBSP	Electron BackScatter Pattem (= BKP)
ECP	Electron Channeling Pattern
ED	Energy Dispersive
EDS	Energy Dispersive X-ray Spectroscopy
MBD	MicroBeam electron Diffraction
MODF	MisOrientation Distribution Function
ODF	Orientation Distribution Function, Orientation Density Function
RHEED	Reflection High Energy Electron Diffraction
SAD	Selected Area electron Diffraction
SEM	Scanning Electron Microscope/Microscopy
Σ value	reciprocal value of the fraction of the coincident lattice sites of two superimposed crystal lattices
TEM	Transmission Electron Microscope/Microscopy
TKP	Transmission Kikuchi diffraction Pattem
XRD	X-Ray Diffraction
XSA	X-ray Scanning Apparatur

About the Book

The present volume is based on 20 invited papers by renowned experts in the field of materials, which were presented in the International Symposium on *Materials for the Third Millennium,* held on November 13, 1999 at the Indian Institute of Technology, Kanpur, India. This Symposium was a prelude to the National Metallurgists' Day celebrations and the Annual Technical Meeting of the Indian Institute of Metals. A wide variety of materials and topics were covered in this Symposium, namely electronic materials, non-metallic materials and superconductors, structural materials and intermetallics, novel characterization techniques, interfaces and surfaces and materials and environment. The presentations were focussed on materials requirement for the rapidly changing technologies in the next millennium and basically dealt with the development, processing and application of advanced materials.

About the Editors

Professors R.K. Ray, V.S.R. Murthy and N.K. Batra are in the Department of Materials and Metallurgical Engineering at IIT Kanpur. Professor K.A. Padmanabhan, formerly Director of IIT Kanpur, is now with the Department of Metallurgical Engineering at IIT Chennai. Professor S. Ranganathan is a faculty member in the Department of Metallurgy, Indian Institute of Science at Bangalore.